

Identification of carbohydrates binding to lectins by using surface plasmon resonance in combination with HPLC profiling

Ricardo Gutiérrez Gallego^{1,3,5}, Simon R. Haseley^{2,3,5},
Vincent F. L. van Miegem⁵, Johannes F. G. Vliegthart⁵,
and Johannes P. Kamerling^{4,5}

⁵Bijvoet Center, Department of Bio-Organic Chemistry, Section of Glycoscience and Biocatalysis, Utrecht University, Padualaan 8, NL-3584 CH Utrecht, The Netherlands

Received on February 24, 2003; revised on November 19, 2003;
accepted on December 30, 2003

A new, powerful method is presented for screening the binding in real time and taking place under dynamic conditions of oligosaccharides to lectins. The approach combines an SPR biosensor and HPLC profiling with fluorescence detection, and is applicable to complex mixtures of oligosaccharides in terms of ligand-fishing. Labeling the oligosaccharides with 2-aminobenzamide ensures a detection level in the fmol range. In an explorative study the binding of RNase B-derived oligomannose-type N-glycans to biosensor-immobilized concanavalin A (Con A) was examined, and an affinity ranking could be established for Man₅GlcNAc₂ to Man₉GlcNAc₂, as monitored by HPLC. In subsequent experiments and using well-defined labeled as well as nonlabeled oligosaccharides, it was found that the fluorescent tag does not interfere with the binding and that the optimum epitope for the interaction with Con A comprises the tetramannoside unit Man α 2Man α 6(Man α 3)Man[D₃B(A)4'], rather than the generally accepted trimannoside Man α 6(Man α 3)Man [B(A)4' or 4(4')3]. In a similar experimental setup, the interaction of various fucosylated human milk oligosaccharides with the fucose-binding lectin from *Lotus tetragonolobus purpureus* was studied, and it appeared that oligosaccharides containing blood group H could selectively be retained and eluted from the lectin-coated surface. Finally, using the same lectin and a mixture of O-glycans derived from bovine submaxillary gland mucin, minor constituents but containing fucose could selectively be picked from the analyte solution as demonstrated by HPLC profiling.

Key words: HPLC profiling/interaction/lectins/
oligosaccharides/surface plasmon resonance

Introduction

Carbohydrates, present as free oligosaccharides or as glycoconjugates, play an important role in many biological events (Dwek, 1996; Varki, 1993). By interacting with carbohydrate-binding proteins, for example, lectins or antibodies, they either promote or prevent cellular adhesion processes. Insight in these carbohydrate-mediated interactions requires detailed knowledge about the carbohydrate structures involved and the precise mechanisms underlying the interactions. Significant advances have been made with the development and application of techniques like chemically induced dynamic nuclear polarization nuclear magnetic resonance (CIDNP-NMR) (Siebert *et al.*, 1997), isothermal titration calorimetry (Doyle, 1997), glycoaffinity chromatography (Caron *et al.*, 1998), affinity capillary electrophoresis (Heegaard *et al.*, 1998), surface plasmon resonance (SPR) (Haseley *et al.*, 1999), and frontal affinity chromatography (Hirabayashi *et al.*, 2000). Most of these techniques allow the evaluation of kinetic parameters of the interaction, but all require the use of purified, well-defined carbohydrate structures. Biologically interesting glycoconjugates are often available in limited amounts only or in mixtures of compounds. This has prompted the search for highly sensitive techniques for the analysis of carbohydrate structures, either obtained directly from complex matrices or after partial purification. Improvements in the fields of chromatography and capillary electrophoresis have made it possible to develop these techniques as predictive, ultra-sensitive profiling methods, especially when combined with fluorescent tagging (Anumula and Dhume, 1998; Liu *et al.*, 1991; Royle *et al.*, 2002; Rudd *et al.*, 1997; Starr *et al.*, 1996). Many of the available fluorescent probes (reviewed in Rice, 2000; Anumula, 2000) allow low fmol detection levels, quantification, and, importantly, do not significantly alter the physical properties of the carbohydrates. In combination with external (Guile *et al.*, 1996) or internal (Charlwood *et al.*, 1999) standards and sequential exoglycosidase digestions, carbohydrate chains can be analyzed in detail (Royle *et al.*, 2002; Rudd *et al.*, 1997, 1999).

In this study the potential of SPR to monitor interactions taking place in solution under dynamic conditions at lectin-coated surfaces was combined with the resolving power of high-performance liquid chromatography (HPLC) for the detection of fluorescently labeled (2-aminobenzamide; 2AB) high-affinity carbohydrate epitopes from complex mixtures. In the development of the method, oligomannose-type N-glycans binding to concanavalin A (Con A) were used. With the authentic mixture of glycans, derived from RNase B, and in a single experiment the

¹Present address: Municipal Institute of Medical Research, Department of Experimental and Health Sciences, University Pompeu Fabra, c/o Doctor Aiguader 80, 08003-Barcelona, Spain

²Present address: CBS Porton Down, DSTL, Salisbury SP4 0JQ, United Kingdom

³These authors contributed equally to this article.

⁴To whom correspondence should be addressed; e-mail: j.p.kamerling@chem.uu.nl

preferential binding of Man₇GlcNAc₂ (Man7), Man₈GlcNAc₂ (Man8), and Man₉GlcNAc₂ (Man9) could be demonstrated. These findings were corroborated employing well-defined structures and are in agreement with earlier observations (Mega *et al.*, 1992), thus validating this approach. Subsequently, using the fucose-binding lectin from *Lotus tetragonolobus purpureaus* (LTA) and a mixture of fucosylated milk oligosaccharides, the selectivity and sensitivity of the combination method was demonstrated. Finally, the experimental setup was exploited to identify fucose-containing oligosaccharides in complex O-glycan mixtures derived from bovine submaxillary gland mucin.

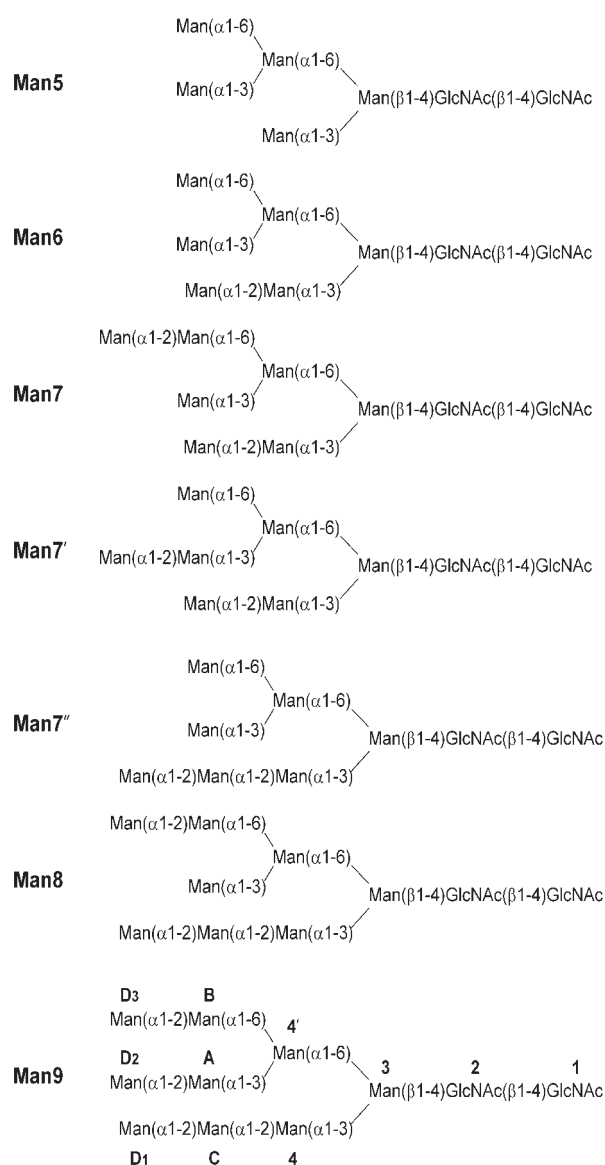


Fig. 1. The oligomannose-type structures from RNase B used in this study. The Man9 structure contains the commonly used codes for the residues.

Results







The combination of SPR and HPLC for carbohydrate ligand fishing

The HPLC profile of 2AB-labeled oligomannose-type N-glycans (not shown) as released from RNase B revealed the presence of Man₅GlcNAc₂ (Man5), Man₆GlcNAc₂ (Man6), Man₇GlcNAc₂ (Man7/7'/7''), Man₈GlcNAc₂ (Man8), and Man₉GlcNAc₂ (Man9) (Figure 1) in a molar ratio of 53.5:22.0:6.6:13.2:4.7 (Table I).

Con A was immobilized at the surface (~8000 response units [RU]) at pH 4.5, at which the lectin associates as a dimer (Gupta *et al.*, 1997) to avoid cooperative binding of the ligands with Con A tetramer. However, to avoid any effects of low pH, the binding experiments were performed at pH 7.4 (physiological pH). Furthermore, the average density of Con A was calculated to correspond to Con A dimers occurring every 100 Å (BIA technology Handbook, 1994) on the surface, minimizing the possibilities of ligand bridging between two adjacent Con A dimers. A sample (50 µl) of 2AB-labeled oligomannose-type N-glycans, containing approximately 1.5 pmol carbohydrate in total, was injected across the Con A surface at a flow rate of 5 µl/min (Figure 2A), collecting the flow-through fraction (injection; fraction B). Subsequently buffer was flowed across for 18 min, during which three fractions (30 µl each) were collected (wash 1–3; data not shown). Finally, the surface was regenerated using 2, 5, and 2 × 10 mM methyl α-D-mannopyranoside (15 µl each), collecting the four effluents (regeneration 1–4; fractions C–F). After filtration and lyophilization, collected fractions B–F were profiled on HPLC using solvent gradient 1. The chromatogram of fraction B (Figure 2B) was nearly identical to that of the starting mixture, as reflected by the relative peak intensities (Table I).

It turned out that during the washing procedure most bound material was retained on the surface. The intensities of the individual peaks in the profiles of the regeneration

Table I. Oligomannose-type structures as present on RNase B

Structure		GU value	Mol %					
			N	I	R1	R2	R3	R4
Man5		6.12	53.5	53.6	35.2	10.3	0.0	0.0
Man6		7.01	22.0	23.6	15.7	16.7	17.4	0.0
Man7'/7''		7.79	6.6	5.9	12.7	-	-	-
Man7		7.97				16.7	19.8	23.6
Man8		8.82				13.2	12.0	26.6
Man9		9.57	4.7	4.8	9.8	17.2	20.4	25.5

Symbols: ●, ²AB, 2AB labelled GlcNAc; ●, β-GlcNAc; ◆, α- or β-Man.

Mol percentages are given for the compounds in the original mixture (N), injection (I), and four regenerations (R1–R4) after the SPR experiment. The values of Man7, Man7', and Man7'' for N, I, and R1 represent the sum of the three isoforms, whereas those for R2 to R4 represent that of Man7 only (isoform retained by Con A).

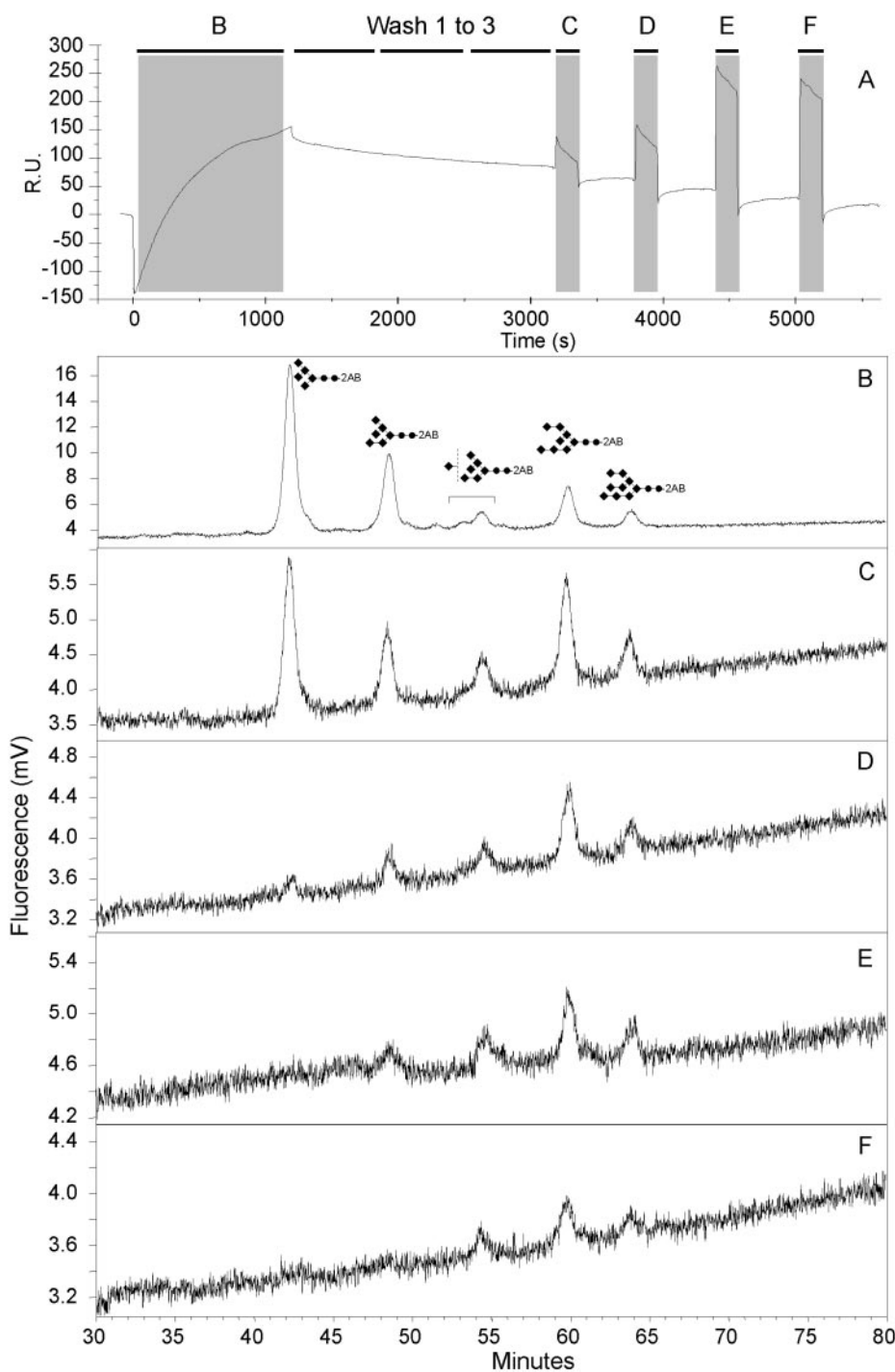


Fig. 2. SPR combined with HPLC analysis of 2AB-labeled oligomannose-type structures interacting with Con A. (A) Sensorgram; (B) injection (representing only 20% of the amount of material recovered during injection); (C) regeneration 1 (2 mM methyl α -D-mannopyranoside); (D) regeneration 2 (5 mM methyl α -D-mannopyranoside); (E, F) regeneration 3 and 4 (10 mM methyl α -D-mannopyranoside). Dots with 2AB, 2AB-labeled GlcNAc; plain dots, β -GlcNAc; diamonds, α - or β -Man (see Figure 1). It should be noted that because the regeneration steps are performed using a large molar excess with respect to the amount of 2AB-labeled material injected, the sensorgram readouts in these steps are not directly related to the corresponding HPLC profiles. This holds for Figures 4, 7, and 8 as well.

(fractions C–F in Figure 2C–F) represented between 20 and 100 fmol per peak. The relative intensities of the individual peaks (Figure 2C–2F) reflected the affinity of the corresponding oligomannose-type structure for Con A.

In Figure 3 and Table I, the relative amounts of each structure in the individual fractions are shown with respect to the initial composition (N). The relative amounts of Man5 and Man6 remain unaltered or show a slight increase in

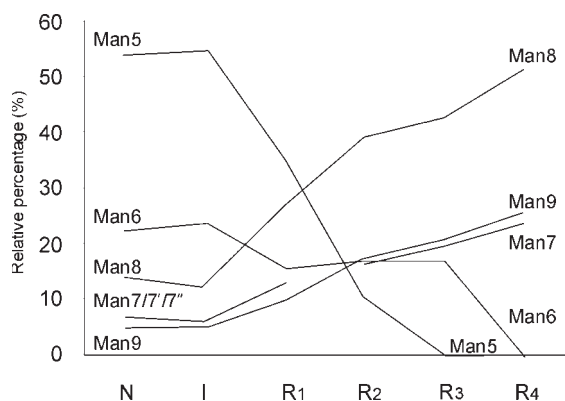


Fig. 3. Changes in the relative percentages (mol) of Man5 to Man9 in the subsequent SPR steps (N, native; I, Injection; R1 to R4, regenerations 1 to 4). Because Man7, Man7', and Man7'' are not completely resolved in the HPLC chromatogram, the values for N, I, and R1 represent the sum of the three isoforms, whereas those for R2 to R4 represent that of Man7 only (isoform retained by Con A).

the flow-through fraction (I), whereas those of Man7/7'/7'', Man8, and Man9 appear to remain unaltered or decrease slightly. Even though only ~10% of the injected material had interacted with the Con A surface, the trend indicated that Man5 and Man6, the major constituents in the mixture, have a lower affinity for Con A than the other components. This observation is clearly corroborated in the four regeneration fractions (R1 to R4) with the incessant increase of the relative amounts of Man7, Man8, and Man9 and the decrease to baseline level of Man5, Man6, and Man7/7'/7''.

The distinction between the binding of the three Man₇GlcNAc₂ structures to Con A was concluded after using isolated structures. These results clearly reveal the usefulness of this approach for the identification of high-affinity ligands directly from a mixture. Moreover, by selecting the appropriate regeneration conditions, an affinity ranking can be established. Although Man5 was present in a 10-fold excess over Man9 in the mixture, the higher affinity of the latter could easily be demonstrated in this experiment. It highlights the fact that even the presence of an excess of a structure or structures, that only display non- or less specific interactions, does not interfere with the ligand fishing.

To more accurately evaluate the interaction of oligomannose-type N-glycans with Con A, oligosaccharides Man5, Man6, Man7/7'/7'', Man8, and Man9 (Figure 1) were isolated, 2AB-labeled, mixed in equimolar amounts, and investigated by SPR combined with HPLC (Man7 was not included). The HPLC profiles (solvent gradient 2) of the collected fractions during the SPR experiment are depicted in Figure 4. The injection (Figure 4A) and three wash fractions (Figure 4B–D) showed a gradual decrease of all peaks. Evaluation of the material dissociated from the Con A surface during regeneration (Figure 4E–H), via the fluorescence of the signals in the HPLC profiles showed that significantly more Man8 and Man9 bound to the Con A surface (total amount of material in regeneration Man8/Man9:Man5/Man6/Man7/7'/7'' ~2:1). Man5, Man6, and

Man7/7'/7'' glycans were completely removed from the surface following the first regeneration step with 2 mM methyl α -D-mannopyranoside (Figure 4E), whereas Man8 and Man9 were only slowly washed from the surface using 10 mM methyl α -D-mannopyranoside (Figure 4G–H). A separate experiment with Man7 and Man7',7'' illustrated that Man7 bound preferentially to Con A. On regeneration of the surface with 2 mM methyl α -D-mannopyranoside, Man7' and Man7'' were efficiently and completely removed from the surface. In the case of Man7, regeneration with 10 mM methyl α -D-mannopyranoside was not sufficient to completely remove Man7 from the Con A surface. It is therefore evident that Man7 does indeed contain the high-affinity epitope present in Man8 and Man9 that is absent in Man7' and Man7''.

Evaluation of the interaction kinetics of Man₅₋₉GlcNAc₂-Con A binding

The kinetics of the interaction between the isolated oligomannose-type glycans Man5 to Man9 (using free and 2AB-labeled compounds) and Con A were performed at a surface containing a low amount of immobilized dimeric lectin (~150 RU, bound at pH 4.5; less than 1 Con A molecule every 1000 Å). The phenomenon of mass transport was assessed by using a standard protocol (Myszka, 1999). By saturating the Con A surface with each of the isolated oligosaccharides in separate experiments and recording the level of response in each sensorgram, co-operative binding effects could be completely ruled out. The gradual increase in SPR response from Man5 (10 RU) to Man9 (20 RU) is indicative of comparable surface coverage, the response being linearly dependent on the molecular mass of the glycan, demonstrating a similar concentration of bound material in each case. Divalent binding would reduce the number of bound molecules by two, and for example Man9 would have produced a response of ~10 RU.

The sensorgrams for the binding of each nonlabeled sample are shown in Figure 5. Differences between the binding characteristics of Man5, Man6, and Man7/7'/7'' on the one hand, and Man7, Man8, and Man9 on the other, are the slower association and dissociation (shallower slope of the curves) of the latter structures. Similar sensorgrams and kinetics were also obtained for the corresponding 2AB-labeled oligomannose-type structures (Figure 6). A comparison of both labeled and unlabeled Man6 and Man9 at identical concentrations proved that the 2AB-label does not influence the interaction between the oligomannose-type structures and Con A. Calculation of the kinetics by fitting the sensorgram to a 1:1 Langmuir binding profile produced χ^2 values with a good fit for the binding of Man5, Man6, and Man7/7'/7'' and K_A values of between $1-3 \times 10^5 \text{ M}^{-1}$ (Table II). The other sensorgrams, that is, those of Man7, Man8, and Man9, proved more difficult to fit to the usual binding models as generated by the BIAevaluation software, however it was clear from the sensorgrams that a more stable complex was formed. The typical structural difference between the group of Man7/Man8/Man9 structures as compared to the group of Man5/Man6/Man7/7'/7'' is the presence of a Man-D₃ unit at the B(A)₄' fragment. An explanation for the poor fit to usual binding models

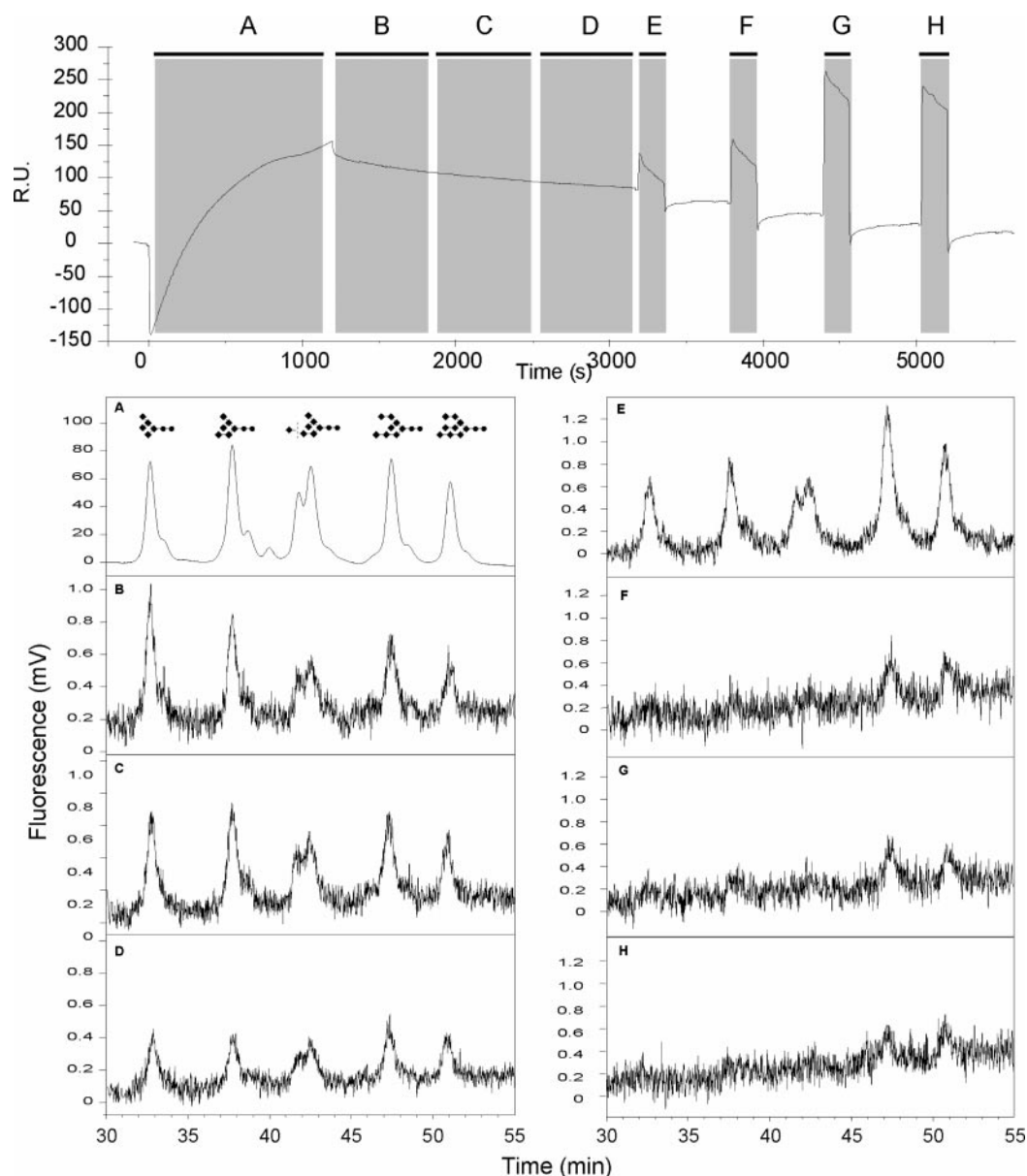


Fig. 4. Top: SPR analysis of the 2AB-labeled oligomannose-type structures Man5 to Man9 (molar ratio 1:1) interacting with Con A; the letters indicate the different SPR steps. (A) recovery; (B) wash 1; (C) wash 2; (D) wash 3; (E) regeneration 1 (2 mM methyl α -D-mannopyranoside); (F) regeneration 2 (5 mM methyl α -D-mannopyranoside); (G) regeneration 3 (10 mM methyl α -D-mannopyranoside); (H) regeneration 4 (10 mM methyl α -D-mannopyranoside). Bottom: HPLC analysis of the different SPR steps. Explanation of the symbols: dots with 2AB, 2AB-labeled GlcNAc; plain dots, β -GlcNAc; diamonds, α - or β -Man (see Figure 1).

could include a distortion of the glycosidic bond between Man-D₃ and Man-B. An analogous suggestion has been made for Man α 6(Man α 3)Man extended with a GlcNAc residue (Moothoo and Naismith, 1998). An approximation of the kinetics indicated Man7, Man8, and Man9 to have a 10-fold higher affinity (K_A $1-3 \times 10^6$ M⁻¹) than Man5, Man6, and Man7'/7'' (K_A $1-3 \times 10^5$ M⁻¹), with the increase in affinity most likely originating from the lower dissociation rates recorded (Table II). As expected, the Man7'/7'' mixture has similar binding characteristics to Man5 and Man6, whereas Man7 has a similar profile to Man8 and Man9. In addition to the care taken to avoid possible

cooperative binding effects at the Con A surface, the higher-affinity binding of Man7 cannot have been caused by this phenomenon because only the high- [Man- α 2Man α 6(Man α 3)Man, D₃B(A)4'] but not the low- (Man- α 2Man α 2Man, D₁C4) affinity oligomannose binding site epitope (Mandal and Brewer, 1993; Mandal *et al.*, 1994) is present in this molecule (Figure 1).

Milk oligosaccharides interacting with LTA lectin

Using the fucose-binding LTA lectin and a mixture of 2AB-labeled oligosaccharides (Figure 7B), isolated from human

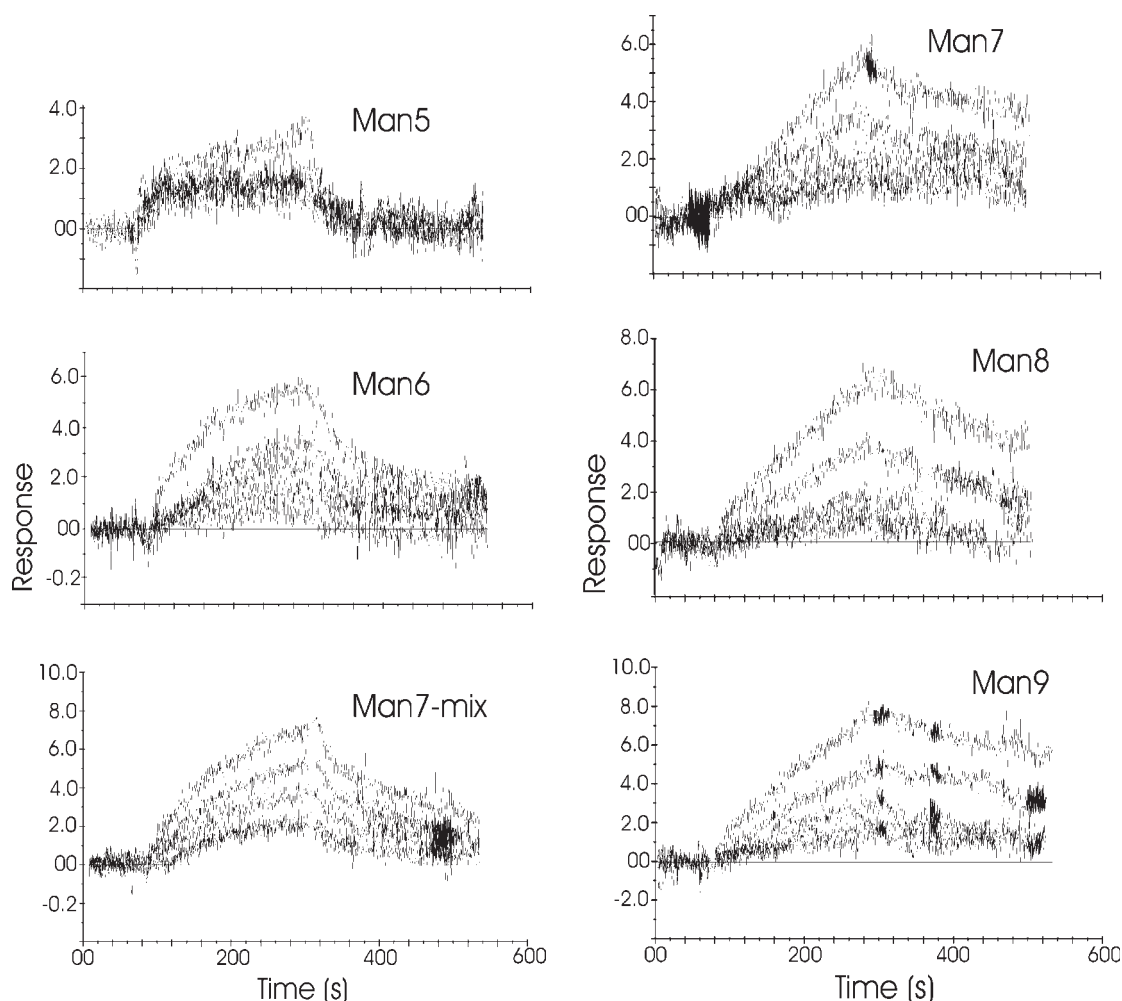


Fig. 5. SPR analysis of isolated oligomannose-type N-glycans. Five different concentrations of oligosaccharides were used in each experiment: 6.25, 12.5, 25, 50, and 100 mM. Man7/7'' represents a mixture of Man7' and Man7'' as depicted in Figure 1. The kinetic data derived from these analyses are summarized in Table II.

milk, a similar SPR experiment as for the Con A system was set up. The components in the mixture have been analyzed by monosaccharide analysis, NMR, mass spectrometry, and HPLC profiling in combination with exoglycosidase digestions (Gutiérrez Gallego, 2001; Haseley *et al.*, 1998).

For the SPR experiment, a solution of the 2AB-labeled milk oligosaccharides (~2 pmol) was injected across the surface at a flow rate of 5 μ l/min for 10 min, during which the flow-through fraction was collected (injection; fraction C in Figure 7A). Subsequently, the system was washed with buffer for 24 min, collecting two fractions (wash 1 and wash 2; fractions D and E in Figure 7A). Finally, regeneration was performed with 2 mM methyl α -L-fucopyranoside (40 μ l), followed by 10 mM methyl α -L-fucopyranoside (40 μ l) to yield regenerations 1 and 2, respectively (fractions F and G in Figure 7A). All fractions collected were filtered, lyophilized, and profiled on HPLC using solvent gradient 3. The HPLC profiles of the isolated milk oligosaccharides prior to SPR experiments (Figure 7B) and of the injection (Figure 7C) showed subtle differences, as demonstrated on integration of the peaks (Table III).

A comparison of the relative peak areas, representing the absolute amounts of different oligosaccharides, indicated that the structures lacking fucose or carrying fucose α -1, 3/4-linked to *N*-acetylglucosamine were more prominent in the injection. This implied that these oligosaccharides had no or weaker interaction with the lectin than the oligosaccharides containing fucose α -1,2-linked to galactose. During the washing procedure, most bound material was retained on the surface (Figure 7D, E). The HPLC profile of the first regeneration fraction (Figure 7F) showed the increase in relative peak areas (Table III) of the structures containing fucose α -1,2-linked to galactose and the absence of structures lacking fucose. These findings are consistent with the specificity of the LTA lectin, exhibiting an increased affinity for the blood group H determinant Fuc(α 1-2)Gal and an especially high affinity for the Fuc(α 1-2)Gal(β 1-4)GlcNAc fragment (Pereira and Kabat, 1974).

In the HPLC profile of regeneration 2, using 10 mM methyl α -L-fucopyranoside, only traces of the most abundant peak (2-fucosyl-lacto-*n*-hexaose) were evident

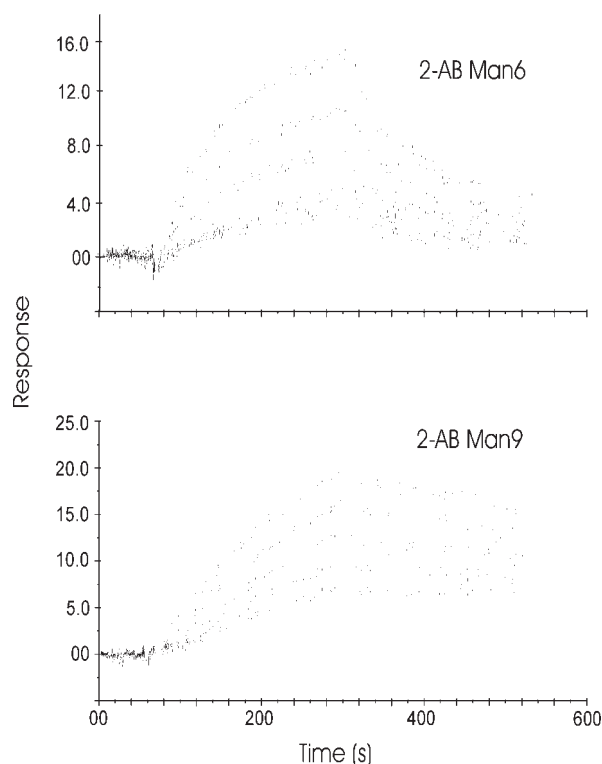


Fig. 6. SPR analysis of 2AB-labeled Man6 and Man9. Five different concentrations of oligomannose-type structures were used in each experiment: 6.25, 12.5, 25, 50, and 100 mM.

Table II. Association and dissociation constants derived from SPR experiments, using immobilized Con A and flowing the various oligomannose-type structures across

Structure		$K_A^* (M^{-1}) * 10^5$	$k_d (s^{-1}) * 10^{-3}$
Man5		1-3	6.1
Man6		1-3	6.5
Man7/7''		1-3	5.0
Man7		10-30	2.4
Man8		10-30	1.8
Man9		10-30	1.4

* Values for K_A are given within a range due to the association kinetics that could only be approximated

All experiments were performed at 25°C.

(Figure 7G), indicating almost complete regeneration of the surface with 2 mM methyl α -L-fucopyranoside. Repetitive experiments yielded identical results, validating the sensitivity, accuracy, and potential of the combination of SPR and

HPLC profiling. In addition, these experiments show that even if no appropriate regeneration conditions are available, a comparison of the HPLC profiles from the native mixture and the injection would allow a prediction of the interacting structure.

Bovine submaxillary gland mucin type I O-glycans interacting with LTA lectin

Using the same fucose-binding lectin, the SPR behavior of a mixture of 2AB-labeled O-glycans from bovine submaxillary gland mucin type I (BSM-I) was studied. The O-glycans have been previously isolated and characterized by NMR spectroscopy as their corresponding alditols (Chai *et al.*, 1992). Using the NMR data and published glucose unit (GU) values for 2AB-labeled O-linked glycans (Mattu *et al.*, 1998; Royle *et al.*, 2002; Rudd *et al.*, 1999), several peaks in the HPLC profile could be assigned. The HPLC profile (solvent gradient 3) of the original mixture of O-glycans and the injection fraction (~2 pmol of carbohydrate were injected) were identical (Figure 8B, C). In the two subsequent washing steps, residual material was washed away (Figure 8D, E). The HPLC profile of the first regeneration step, employing 2 mM methyl α -L-fucopyranoside (40 μ l), showed four major peaks (a–d in Figure 8F) with an intensity order of $d > b > a > c$. The second regeneration step, using 10 mM methyl α -L-fucopyranoside (40 μ l), contained the same four peaks but with an intensity order of $a > b > d > c$ (Figure 8G). The sum of the peaks from both regeneration steps represented ~1% (50–100 fmol) of the total amount of material used for the SPR experiment, and the elution positions of a–d corresponded to elution positions of minor components in the original profile (Figure 8B). Based on the elution positions (GU values) of peaks a–d, they could not belong to difucosylated core 2 type {GlcNAc(β 1-6)[Gal(β 1-3)]GalNAc} or core 3 type [GlcNAc(β 1-3)GalNAc] structures.

Using this restriction, the NMR data (Chai *et al.*, 1992) and the observed differences in affinity for peaks a–d, it is evident that peaks a–d correspond to relatively short glycans containing fucose residues and that the linkage type is most likely different in peaks a and b (α -1,2-) when compared to d (α -1,3-). This approach not only allowed the identification of fucose-containing structures that might have been ignored if conventional techniques had been used but also permitted direct quantification of glycans in a mixture. The combination of the SPR and HPLC approach may prove particularly valuable for identifying trace amounts of epitopes responsible for specific interactions as, for example, the inhibition of *Escherichia coli* adhesion by a fuco-oligosaccharide present in milk at a concentration of 20 pmol/L (Cravioto *et al.*, 1991).

Discussion

The combination of an SPR biosensor and HPLC with fluorescent detection provides a powerful profiling technique capable of ligand fishing (oligosaccharides) and ordering the binding of oligosaccharides to complementary molecules according to affinities. In the development

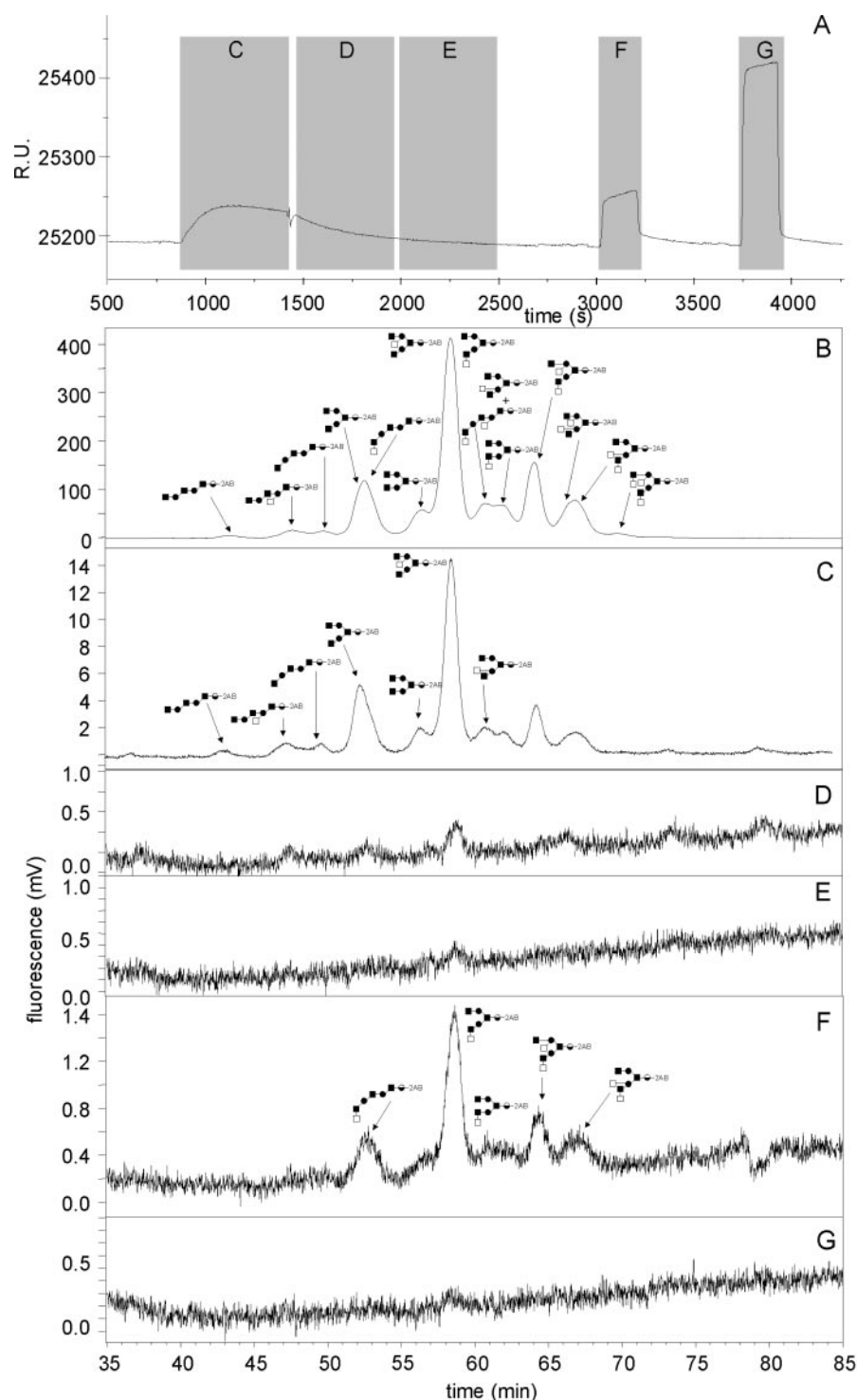
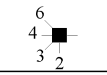

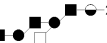
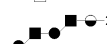







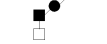






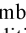
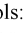
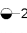
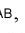
Fig. 7. SPR combined with HPLC analysis of 2AB-labeled milk oligosaccharides (HB1) interacting with the LTA lectin. (A) Sensorgram; (B) untreated mixture (~15 pmol); (C) injection (representing only 20% of the amount of material recovered during injection); (D) wash 1; (E) wash 2; (F) regeneration 1 (2 mM methyl α -L-fucopyranoside); (G) regeneration 2 (10 mM methyl α -L-fucopyranoside). Explanation of the symbols and the graphical linkage types is given in Table III.

of the presented approach, different oligosaccharide-lectin combinations were successfully examined. The system is very sensitive (fmol) and suitable for selecting particular structures from a mixture, even when present as minor

constituents. In addition, the method can be used for the detection and characterization of unknown carbohydrate-binding molecules, present at the surface of intact microorganisms (Gutiérrez Gallego, 2001).

Table III. GU values for the 2AB-labeled milk oligosaccharides from HB1

Structure 	GU value	% (mol)		
		Native	Recovery	Regen.1
 2AB	4.47	-	-	-
 2AB	4.89	2.1	4.2	-
 2AB	5.13	1.4	2.9	-
 2AB	5.41	13.9	18.0	19.6
 2AB	5.49			
 2AB	5.81	5.4	6.1	4.9
 2AB	6.10	38.7	36.9	43.7
 2AB	6.10			
 2AB	6.38	6.5	6.4	2.4
 2AB	6.38			
 2AB	6.51	6.5	4.9	2.7
 2AB	6.73	14.1	9.3	14.1
 2AB	7.05	10.6	7.6	12.7
 2AB	7.13			
 2AB	7.48	-	-	-

Symbols:  2AB, 2AB labelled Glc;  β -Gal;  β -GlcNAc;  α -Fuc.
In addition, mol percentages are given of each identified structure present in the HPLC profile of the native mixture, the injection, and regeneration 1.

In the oligosaccharide–Con A study, oligomannose-type glycans were allowed to compete for the binding sites on Con A in a dynamic situation, and the course of interaction was quantitatively monitored. We observed that the monovalent interaction of oligomannose-type structures containing the Man α 2 unit D₃ connected to Man-B of the B(A)₄' fragment has a higher affinity for the binding site of dimeric Con A than that of the B(A)₄' structure alone, and therefore the optimum binding epitope is actually this tetrasaccharide unit (Figure 1); a preliminary communication about the ranking of Man₅GlcNAc₂ to Man₉GlcNAc₂ has appeared (Haseley *et al.*, 2001). Over the past 20 years, the specificity and the thermodynamics of interaction of Con A have been studied extensively (e.g., Clegg *et al.*, 1981; Dam *et al.*, 2000; Derewenda *et al.*, 1989; Goldstein *et al.*, 1974; Goldstein and Poretz, 1986; Gupta *et al.*, 1997; Mandal and Brewer,

1993; Mandal *et al.*, 1994; Mega *et al.*, 1992). These studies have disclosed the different affinities that mono- (K_A 8.2×10^3 M⁻¹), di- ($K_A \sim 4 \times 10^4$ M⁻¹) and trisaccharides (K_A 1.5 – 3.4×10^5 M⁻¹) built up from mannose display toward Con A. Crystallographic studies of the binding of well-defined oligosaccharides to Con A (Bouckaert *et al.*, 1999; Moothoo and Naismith, 1998; Moothoo *et al.*, 1999; Naismith and Field, 1996) revealed that the binding site is an elongated cleft on the surface of the protein. This site is sufficiently large to accommodate a pentasaccharide [GlcNAc β 2Man α 6(GlcNAc β 2Man α 3)Man: K_A 1.4×10^6 M⁻¹], flexible enough to allow the binding of a Man α 2Man α OMe unit in two different ways, and requires at least one monosaccharide in the appropriate orientation to allow interactions with Asn-14, Leu-99, Tyr-100, Asp-208, and Arg-228 of Con A. It is generally assumed that the high-affinity binding epitope for Con A consists of a trisaccharide [B(A)₄' or 4(4')3].

Using pyridylamino-derivatized oligosaccharides Mega *et al.* (1992) conducted a study employing microequilibrium dialysis at pH 7.0 followed by HPLC. Our observations concord with their findings in the identification of the contribution of Man-D₃ to the increased affinity and of the order of magnitude for the difference in affinity between oligomannose-type structures containing the D₃B(A)₄' epitope and those without. However, it is very likely that the reported K_A values reported in that study are overestimated by a factor of 3–5, judging from other literature data and our own results; also, they could not completely rule out cooperative binding as the experiments were performed with tetrameric Con A.

In view of differences between our observations, in agreement with one other report (Mega *et al.*, 1992) and other literature, it was decided to examine the interaction between Con A and different oligomannose-type structures in more detail. The first and most important item to rule out was that of cooperative binding events at the surface of the SPR biosensor. To avoid the appearance of cooperative binding, Con A was immobilized to the SPR sensor chip at pH 4.5, at which the lectin associates as a dimer. In this way divalent binding, as has been reported for the interaction to the tetramer, could be avoided. However, to exclude any effects of a lower pH on the interaction, the glycan–lectin binding experiments were performed at a physiological pH. The lectin was immobilized with a low level (150 RU) of Con A, representing less than one Con A molecule every 1000 Å, so that the possibility of a glycan bridging two Con A dimers could be completely ruled out. Moreover, it was shown that saturation of the surface with Man₅ to Man₉ brought about a gradual increase of the maximum response level, a result in agreement with the absence of cooperative binding events. Finally, the higher-affinity binding of Man₇ but not of Man₇' and Man₇'' confirmed that the difference in affinity was a result of binding at one binding site.

The conformation of the lectin has not been changed by immobilization to the surface because the calculated affinities are in agreement with those reported by using other methods (Dam *et al.*, 1998, 2000; Gupta *et al.*, 1997; Mandal and Brewer, 1993; Mandal *et al.*, 1994). Finally, the possible effect of the 2AB label in the initial experiments

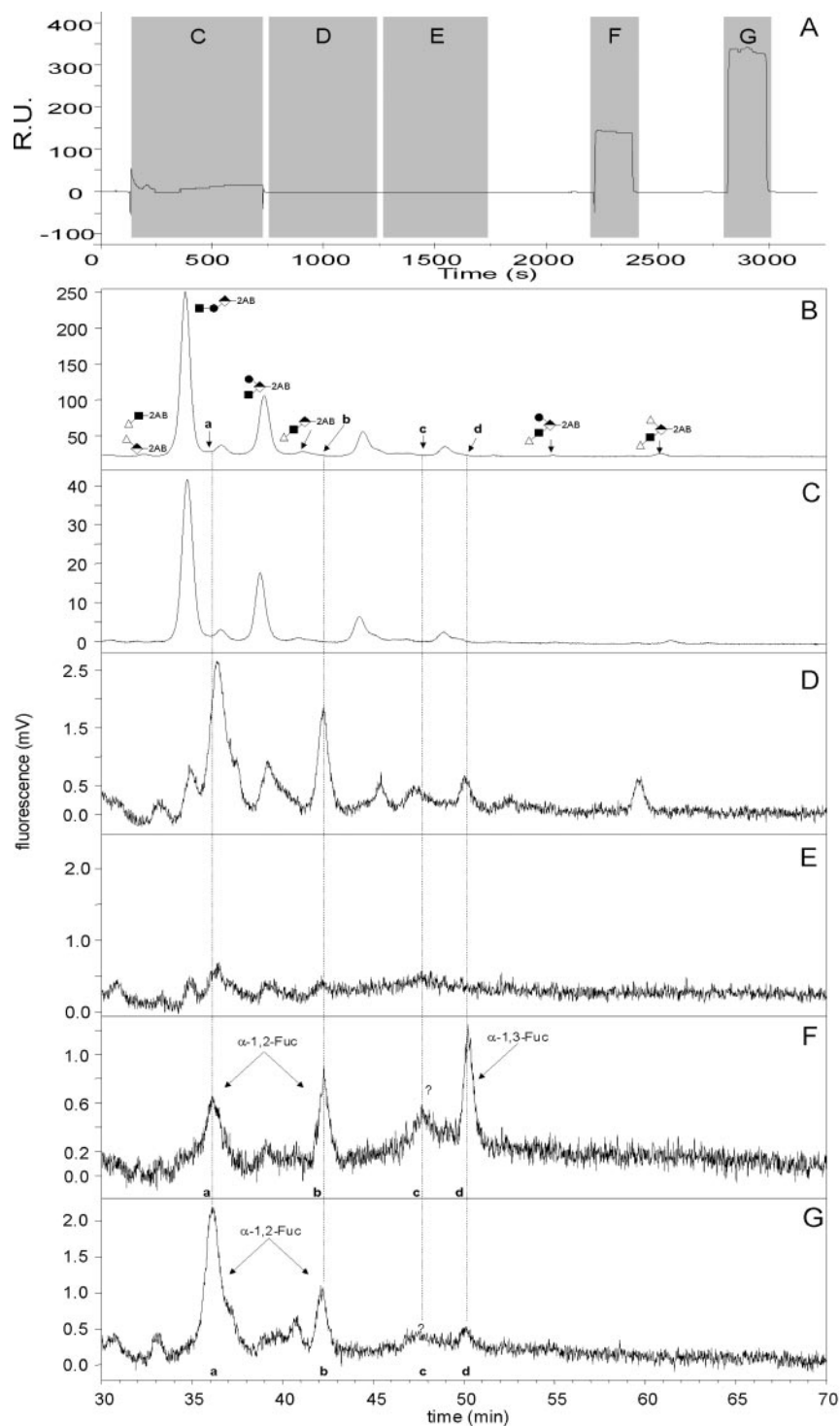


Fig. 8. SPR combined with HPLC analysis of 2AB-labeled BSM-I O-glycans interacting with the LTA lectin. (A) Sensorgram; (B) native mixture (~5 pmol); (C) injection (representing only 20% of the amount of material recovered during injection); (D) wash 1; (E) wash 2; (F) regeneration 1 (2 mM methyl α -L-fucopyranoside); (G) regeneration 2 (10 mM methyl α -L-fucopyranoside). Half-shaded diamonds with 2AB, 2AB-labeled GalNAc; dots, β -GlcNAc; closed squares, β -Gal; open squares, α -Fuc; triangles, α -Neu5Ac. For graphical linkage types information, see Table III.

was completely ruled out by observing identical kinetics of labeled and nonlabeled glycans.

In conclusion, we suggest here that the $\text{Man}\alpha 2\text{Man}$ element in $\text{D}_3\text{B(A)}4'$, present in Man_7 to Man_9 , binds in a

fashion similar to the $\text{GlcNAc}\beta 2\text{Man}\alpha 6$ epitope in the pentasaccharide $\text{GlcNAc}\beta 2\text{Man}\alpha 6(\text{GlcNAc}\beta 2\text{Man}\alpha 3)\text{Man}$ (Moothoo and Naismith, 1998), thereby contributing significantly to the higher affinity. We propose the optimum

Table IV. Proton chemical shifts (referenced to internal acetone, δ 2.225) of the oligomannose-type N-glycans, isolated from RNase B, recorded at 300 K in D₂O

Proton H1	Man5	Man6	Man7	Man7'	Man7''	Man8	Man9
GlcNAc-1 α	5.189	5.187	5.187	5.188	5.188	5.187	5.189
Man-4	5.095	5.346	5.347	5.340	5.340	5.338	5.330
Man-4'	4.870	4.870	4.869	4.870	4.870	4.868	4.869
Man-A	5.093	5.092	5.089	5.406	5.092	5.087	5.400
Man-B	4.906	4.907	5.145	4.907	4.907	5.145	5.139
Man-C	—	5.051	5.053	5.055	5.303	5.303	5.304
Man-D1	—	—	—	—	5.042	5.042	5.047
Man-D2	—	—	—	5.056	—	—	5.058
Man-D3	—	—	5.042	—	—	5.042	5.047

binding carbohydrate epitope of Con A to be Man α 2 Man α 6(Man α 3)Man [D₃B(A)4', Figure 1], rather than the Man α 6(Man α 3)Man structure [B(A)4']. The tetrasaccharide does not appear to bind via a simple 1:1 interaction model but is more likely to undergo a conformational change to incorporate the mannose D₃ residue. Interestingly, Bachhawat *et al.* (2001), using SPR, noted a comparable binding phenomenon between oligomannose-type structures (free oligosaccharides and glycopeptides) and the garlic lectin from *Allium sativum*, although a discrimination between D₃B(A)4' and B(D₂A)4' was not made.

Improvements of the profiling system could involve the development of an SPR surface capable of binding more molecules, which at present is in the picomole to femtomole range. In addition, the implementation of already commercially available micro flow cells in the fluorescence detector could enhance the sensitivity even further. The combination of SPR and HPLC could be interfaced in the future without too many difficulties. The collected SPR fractions never exceeded the maximum injectable volume for the analytical HPLC column; the buffer systems of both techniques are compatible, and no major purification is needed after SPR. Finally, the volatile buffer system applied for the HPLC profiling permits amplification of the system with an in-line coupled mass spectrometer. This would facilitate detailed structural information and further broaden the scope of the technique.

Materials and methods

Chemicals

RNase B (EC 3.1.27.5), Con A, LTA, and BSM-I were purchased from Sigma (St. Louis, MO); and recombinant peptide-N⁴-(N-acetyl- β -glucosaminyl)asparagine amidase F (PNGase F; EC 3.5.1.52) from Roche Diagnostics GmbH, Mannheim, Germany. All other chemicals were of highest purity commercially available.

Preparation of oligosaccharides

N-glycans of RNase B (2 mg) were released by PNGase F digestion as described elsewhere (Van Rooijen *et al.*, 1998). The mixture of liberated oligosaccharides was separated

from detergent, protein, and salts in a single step, on graphitized carbon columns (Packer *et al.*, 1998). The O-glycans of BSM-I (25 mg) were released by manual hydrazinolysis (4 h, 65°C) and further purified as described (Patel *et al.*, 1993). Human milk oligosaccharides were a gift from Prof. H. H. Baer (University of Ottawa, Canada).

Labeling of the glycans

Oligosaccharides were fluorescently labeled with 2AB essentially as described. Briefly, to a solution of 23.6 mg 2AB in 500 μ l dimethylsulfoxide/acetic acid (70:30, v/v) was added 35.4 mg NaCNBH₃, and the mixture was heated for 2 min at 65°C to yield a clear solution. An aliquot (5 μ l) of the solution was added to dried oligosaccharide (P₂O₅), and the mixture was incubated twice for 1 h at 65°C with intermediate mixing. After cooling to room temperature, the mixture was transferred onto an acid-preconditioned QMA strip (3 \times 10 cm), and the residual reagents were eluted from the labeled glycan mixture by ascending chromatography using acetonitrile. The labeled glycan mixture (remaining at the baseline) was excised from the strip, placed in an ultrafree MC centrifugal Eppendorf filter (5000 nmwl), and recovered by centrifugation with water (3 \times 200 μ l, 8000 \times g, 15 min). The resulting solution was lyophilized and redissolved in 100 μ l water; an aliquot was used for SPR and/or HPLC analysis. Quantifications of the 2AB-labeled oligosaccharides are based on 2AB calibration curves.

Isolation, purification, and characterization of oligomannose-type glycans

Oligomannose-type N-glycans were enzymatically released from RNase B (20 mg) using PNGase F and fractionated by high-performance anion exchange chromatography on a Dionex LC system, using a CarboPac PA-1 pellicular anion-exchange column (0.9 \times 25 cm, Dionex, Sunnyvale, CA) and a gradient buffer consisting of 0.1 M NaOH/0.5 M sodium acetate (Van Rooijen *et al.*, 1998). Collected fractions were neutralized with diluted acetic acid, desalted by gel filtration on HiTrap columns (5 \times 5 ml bed volume), then lyophilized. Man5, Man6, Man8, and Man9 were obtained as pure compounds. The Man7 fraction contained 5–10 mol% Man5 and Man6. Man7' and Man7'' (molar

ratio, 2:3) coeluted, and the Man7''/7''' fraction contained ~5 mol% Man8. The structures of the oligosaccharides in each fraction were identified by ^1H -NMR spectroscopy (Table IV) (Hård *et al.*, 1991; Priem *et al.*, 1993; Tseneklidou-Stoeter *et al.*, 1995). Aliquots of the oligosaccharides were fluorescently labeled with 2AB as reported previously (Stroop *et al.*, 2000).

NMR spectroscopy

Prior to analysis, oligosaccharides were repeatedly exchanged in D_2O (99.9 atom % D, Cambridge Isotope Laboratories, Andover, MA) with intermediate lyophilization and finally dissolved in 450 μl D_2O (99.96 atom % D, Isotec). Resolution-enhanced ^1H 1D and 2D NMR spectra were recorded on a Bruker DRX-500 instrument, equipped with a 5 mm TXI-probe, at probe temperatures of 300 K (Department of NMR Spectroscopy, Utrecht University). Chemical shifts (δ) are expressed in ppm relative to internal acetate (δ 1.908, acetone δ 2.225). HOD signal suppression was achieved by applying a WEFT pulse sequence (Hård *et al.*, 1992) in 1D ^1H experiments and by presaturation for 1 s in 2D experiments. 2D total correlation spectroscopy spectra were recorded by using MLEV-17 mixing sequences with effective spin-lock times between 20 and 100 ms. ^1H 1D and 2D spectra were processed on Silicon Graphics IRIS work stations (Indigo 2 and O2) using TRITON software (van Kuik *et al.*, Bijvoet Center, Departments of Bio-Organic Chemistry and NMR Spectroscopy).

SPR

All SPR experiments were performed on a BIAcore 2000 system, using a running buffer (pH 7.4) consisting of 10 mM Tris, 150 mM NaCl, 1 mM CaCl_2 , and 1 mM MgCl_2 . For the experiments, carboxymethylated dextran-coated sensorchips (CM5, Pharmacia, Uppsala, Sweden) were activated (Haseley *et al.*, 1999), and different lectins immobilized. For the preparation of a Con A lectin surface, dimeric Con A (in 10 mM NaOAc, pH 4.5) was attached to all four channels (~8000 RU each). Experiments were performed at a flow rate of 5 $\mu\text{l}/\text{min}$. A solution of the 2AB-labeled Man5 to Man9 (Figure 1) mixture (50 μl) was flowed across the sensor chip (flow cells in series), and the injected sample was recovered manually, while material eluting from the surface by using buffer was collected automatically by the instrument in three fractions of 30 μl each. The surface was regenerated by using 2 mM (15 μl), 5 mM (15 μl), and 2×10 mM (15 μl) methyl α -D-mannopyranoside, and the corresponding fractions were recovered for injection on HPLC. Finally, a regeneration step was carried out using 100 mM methyl α -D-mannopyranoside (40 μl), but the eluent was not collected.

For calculation of the kinetics of interaction of Man5 to Man9 glycans, separate experiments with a set of 2AB-labeled and a set of nonlabeled compounds were performed on a flow cell containing 150 RU of dimeric Con A (active surface). A flow cell containing 150 RU of denatured dimeric Con A was used as a control surface; denaturation was carried out on the chip using 3×40 μl 6 M guanidinium chloride (pH 1.5). The experiments were performed in running buffer at a flow rate of 5 $\mu\text{l}/\text{min}$, as already mentioned.

Oligosaccharide fractions, at concentrations between 6.25 and 100 $\mu\text{mol}/\text{L}$, were injected for 3 min and left to dissociate for a further 3 min. Saturation of the surface was achieved by injecting 1 mM of each isolated oligosaccharide fraction across the surface.

Association and dissociation rate constants (k_a and k_d , respectively), and the equilibrium association constant (K_A) were calculated by nonlinear fitting of the primary sensorgram (BIAevaluation program version 3.0, 1997) data using the BIAevaluation 3.0 software (Pharmacia).

For the preparation of the LTA lectin surface, a similar protocol was used, injecting the lectin solution across the surface for 4 min (20 μl). The resulting response was ~10,000 RU for each of the four surfaces. Regeneration was accomplished by using 2 mM (40 μl) and 10 mM (40 μl) methyl α -L-fucopyranoside.

HPLC profiling

Samples collected during the SPR experiments were directly applied to a ultrafree MC centrifugal Eppendorf filter (5000 nmwl), and centrifuged at $8000 \times g$ for 7 min. Subsequently, the filters were washed with 3×100 μl double distilled water and centrifuged. The pooled effluents were lyophilized, redissolved in 100 μl starting HPLC buffer, and profiled. The HPLC system used for the profiling consisted of a Waters (Milford, CT) 2690 XE module equipped with an in-line degasser, a temperature control unit (maintained at 30°C throughout the experiments) and a 474 scanning fluorescence detector. The system was controlled via a LAC/E interface using Waters Millennium 32 software. The GlycosepN, normal phase HPLC column (4.6×100 mm) was obtained from Oxford Glycosciences. The column was calibrated in GU with a standard mixture of glucose oligomers.

Normal phase HPLC was carried out using the following gradient conditions using 50 mM ammonium formate buffer (pH 4.4; solvent A) and acetonitrile (solvent B): gradient 1 (Figure 2), solvent A and 20% solvent A in solvent B (solvent C) at a flow rate of 0.8 ml/min. Following injection, samples were eluted with a linear gradient of 6.5–44% A over 100 min, followed by a linear gradient of 44–100% A over the next 3 min; gradient 2 (Figure 4), solvent A and solvent B at a flow rate of 0.4 ml/min. Following injection, samples were eluted with a linear gradient of 35–53% A over 92 min, followed by a linear gradient of 53–100% A over the next 3 min. In both cases, the flow rate was increased to 1 ml/min with 100% A over the next 2 min and then for a further 5 min. The system was then reequilibrated to 6.5% A (Figure 2) or 35% A (Figure 4). The total run time was 140 min.

For normal phase HPLC profiling of milk oligosaccharides and O-glycans, the following gradient conditions were used (gradient 3): solvent A was 50 mM ammonium formate (pH 4.4), solvent B was acetonitrile, and the flow rate was 0.4 ml/min. Following injection, samples were eluted by a linear gradient of 20–47.5% A over 120 min, followed by a linear gradient of 47.5–100% A over the next 3 min. Using 100% A the flow rate was then increased to 1 ml/min over the next 2 min, then the column was eluted with 100% A for 5 min and subsequently reequilibrated in 20% A before injection of the next sample. The total run time was 160 min.

Acknowledgments

We kindly acknowledge the gift of milk oligosaccharides by Prof. H.H. Baer from the University of Ottawa (Ontario, Canada). We are also thankful to Drs. P.M. Rudd, T. Mattu, E. Hart, and Prof. R.A. Dwek from the OGBI (Oxford, United Kingdom) for sharing their expertise on O-glycan release, HPLC profiling and the use of PeakTime software. The E.C. is acknowledged for the financial support, project FAIR CT 97–3142, program NOFA.

Abbreviations

2AB, 2-aminobenzamide; BSM-I, bovine submaxillary gland mucin type I; Con A, concanavalin A; GU, glucose units; HPLC, high-performance liquid chromatography; LTA, *Lotus tetragonolobus purpureus* agglutinin; NMR, nuclear magnetic resonance; PNGase F, peptide- N^4 -(*N*-acetyl- β -glucosaminyl)asparagine amidase F; RU, response unit; SPR, surface plasmon resonance.

References

- Anumula, K.R. and Dhume, S.T. (1998) High resolution and high sensitivity methods for oligosaccharide mapping and characterisation by normal phase liquid chromatography following derivatisation with highly fluorescent anthranilic acid. *Glycobiology*, **8**, 685–694.
- Anumula, K.R. (2000) High-sensitivity and high-resolution methods for glycoprotein analysis. *Anal. Biochem.*, **283**, 17–26.
- BIAevaluation program version 3.0. (1997) Pharmacia Biosensor AB, Uppsala, Sweden.
- BIAtechnology Handbook. (1994) Pharmacia Biosensor AB, Uppsala, Sweden, pp. 1–3.
- Bachhawat, K., Thomas, C.J., Amutha, B., Krishnasastri, M.V., Khan, M.I., and Surolia, A. (2001) On the stringent requirement of mannosyl substitution in mannooligosaccharides for the recognition by garlic (*Allium sativum*) lectin. A surface plasmon resonance study. *J. Biol. Chem.*, **276**, 5541–5546.
- Bouckaert, J., Hamelryck, T.W., Wyns, L., and Loris, R. (1999) The crystal structures of Man(α 1-3)Man(α 1-O)Me and Man(α 1-6)Man(α 1-O)Me in complex with concanavalin A. *J. Biol. Chem.*, **274**, 29188–29195.
- Caron, M., Seve, A.-P., Bladier, D., and Joubert-Caron, R. (1998) Glycoaffinity chromatography and biological recognition. *J. Chromatogr. B*, **715**, 153–161.
- Chai, W., Hounsell, E.F., Cashmore, G.C., Rosankiewicz, J.R., Bauer, C.J., Feeney, J., Feizi, T., and Lawson, A.M. (1992) Neutral oligosaccharides of bovine submaxillary mucin. A combined mass spectrometry and ^1H -NMR study. *Eur. J. Biochem.*, **203**, 257–268.
- Charlwood, J., Tolson, D., Dwek, M., and Camilleri, P. (1999) A detailed analysis of neutral and acidic carbohydrates in milk. *Anal. Biochem.*, **273**, 261–277.
- Clegg, R.M., Loontjens, F.G., Van Landschoot, A., and Jovin, T.M. (1981) Binding kinetics of methyl α -D-mannopyranoside to concanavalin A: temperature-jump relaxation study with 4-methylumbelliferyl α -D-mannopyranoside as a fluorescence indicator ligand. *Biochemistry*, **20**, 4687–4692.
- Cravioto, A., Tell, A., Villafan, H., Ruiz, J., Del Vedovo, S., and Neeser, J.-R. (1991) Inhibition of localised adhesion of enteropathogenic *E. coli* to Hep-2 cells by immunoglobulin and oligosaccharide fractions of human colostrum and breast milk. *J. Infect. Dis.*, **163**, 1427–1455.
- Dam, T.K., Oscarson, S., Sacchettini, J.C., and Brewer, C.F. (1998) Differential solvation of “core” trimannoside complexes of the *Dioclea grandiflora* lectin and concanavalin A detected by primary solvent isotope effects in isothermal titration microcalorimetry. *J. Biol. Chem.*, **273**, 32826–32832.
- Dam, T.K., Roy, R., Das, S.K., Oscarson, S., and Brewer, C.F. (2000) Binding of multivalent carbohydrates to concanavalin A and *Dioclea grandiflora* lectin—thermodynamic analysis of the multivalency effect. *J. Biol. Chem.*, **275**, 14223–14230.
- Derewenda, Z., Yariv, J., Helliwell, J.R., Kalb (Gilboa), A.J., Dodson, E.J., Papiz, M.Z., Wan, T., and Campbell, J. (1989) The structure of the saccharide binding site of concanavalin A. *EMBO J.*, **8**, 2189–2193.
- Doyle, M.L. (1997) Characterization of binding interactions by isothermal titration calorimetry. *Curr. Opin. Biotechnol.*, **8**, 31–35.
- Dwek, R.A. (1996) Glycobiology: towards understanding the function of sugars. *Chem. Rev.*, **96**, 683–720.
- Goldstein, I.J. and Poretz, R.D. (1986) Isolation, physicochemical characterization, and carbohydrate-binding specificity of pectins. In Liener, I.E., Sharon, N., and Goldstein, I.J. (Eds.), *The lectins*. Academic Press, New York, pp. 33–247.
- Goldstein, I.J., Reichert, C.M., and Misaki, A. (1974) Interaction of concanavalin A with model substrates. *Ann. NY Acad. Sci.*, **234**, 283–295.
- Gupta, D., Dam, T.K., Oscarson, S., and Brewer, C.F. (1997) Thermodynamics of lectin-carbohydrate interactions. Binding of the core trimannoside of asparagine-linked carbohydrates and deoxy analogs to concanavalin A. *J. Biol. Chem.*, **272**, 6388–6392.
- Guile, G.R., Rudd, P.M., Wing, D.R., Prime, S.R., and Dwek, R.A. (1996) A rapid high-resolution high-performance liquid chromatographic method for separating glycan mixtures and analyzing oligosaccharide profiles. *Anal. Biochem.*, **240**, 210–226.
- Gutiérrez Gallego, R. (2001) Enzymatic synthesis and biomolecular interactions of glycoconjugates. PhD thesis, Utrecht University, Netherlands, pp. 131–162.
- Hård, K., Mekking, A., Kamerling, J.P., Dacremont, G.A., and Vliegthart, J.F.G. (1991) Different oligosaccharides accumulate in the brain and urine of a cat with α -mannosidosis: structure determination of five brain-derived and seventeen urinary oligosaccharides. *Glycoconjugate J.*, **8**, 17–28.
- Hård, K., Van Zadelhoff, G., Moonen, P., Kamerling, J.P., and Vliegthart, J.F.G. (1992) The Asn-linked carbohydrate chains of human Tamm-Horsfall glycoprotein of one male. Novel sulfated and novel *N*-acetylgalactosamine-containing N-linked carbohydrate chains. *Eur. J. Biochem.*, **209**, 895–915.
- Haseley, S.R., Talaga, P., Gutiérrez Gallego, R., Kamerling, J.P., and Vliegthart, J.F.G. (1998) Structural characterisation and profiling of human milk oligosaccharides. XIX International Carbohydrate Symposium, AP006, San Diego, CA.
- Haseley, S.R., Talaga, P., Kamerling, J.P., and Vliegthart, J.F.G. (1999) Characterization of carbohydrate binding specificity and kinetic parameters of lectins by surface plasmon resonance. *Anal. Biochem.*, **274**, 203–210.
- Haseley, S.R., Gutiérrez Gallego, R., McDonnell, M.B., Kamerling, J.P., and Vliegthart, J.F.G. (2001) Exploring biomolecular carbohydrate epitope recognition—a new approach. *Glycoconjugate J.*, **18**, 30.
- Heegaard, N.H.H., Nilsson, S., and Guzman, N.A. (1998) Affinity capillary electrophoresis: important application areas and some recent developments. *J. Chromatogr. B*, **715**, 29–54.
- Hirabayashi, J., Arata, Y., and Kasai, K. (2000) Reinforcement of frontal affinity chromatography for effective analysis of lectin-carbohydrate interactions. *J. Chromatogr. A*, **890**, 261–271.
- Liu, J.P., Shirota, O., Wiesler, D., and Novotny, M. (1991) Ultrasensitive fluorimetric detection of carbohydrates as derivatives in mixtures separated by capillary electrophoresis. *Proc. Natl Acad. Sci. USA*, **88**, 2302–2306.
- Mandal, D.K. and Brewer, C.F. (1993) Differences in the binding affinities of dimeric concanavalin A (including acetyl and succinyl derivatives) and tetrameric concanavalin A with large oligomannose-type glycopeptides. *Biochemistry*, **32**, 5116–5120.
- Mandal, D.K., Kishore, N., and Brewer, C.F. (1994) Thermodynamics of lectin-carbohydrate interactions. Titration microcalorimetry measurements of the binding of N-linked carbohydrates and ovalbumin to concanavalin A. *Biochemistry*, **33**, 1149–1156.
- Mattu, T.S., Pleass, R.J., Willis, A.C., Mogens, K., Wormald, M.R., Lellouch, A.C., Rudd, P.M., Woof, J.M., and Dwek, R.A. (1998) The glycosylation and structure of human serum IgA1, Fab, and Fc regions and the role of N-glycosylation on Fc receptor interactions. *J. Biol. Chem.*, **273**, 2260–2272.

- Mega, T., Oku, H., and Hase, S. (1992) Characterization of carbohydrate-binding specificity of concanavalin A by competitive binding of pyridylamino sugar chains. *J. Biochem.*, **111**, 396–400.
- Moothoo, D.N. and Naismith, J.H. (1998) Concanavalin A distorts the β -GlcNAc-(1 \rightarrow 2)-Man linkage of β -GlcNAc-(1 \rightarrow 2)- β -Man-(1 \rightarrow 3)-[β -GlcNAc-(1 \rightarrow 2)- β -Man-(1 \rightarrow 6)]-Man upon binding. *Glycobiology*, **8**, 173–181.
- Moothoo, D.N., Canan, B., Field, R.A., and Naismith, J.H. (1999) Man α 1-2Man α -OMe-concanavalin A complex reveals a balance of forces involved in carbohydrate recognition. *Glycobiology*, **9**, 539–545.
- Myszka, D.G. (1999) Improving biosensor analysis. *J. Mol. Recognition*, **12**, 279–284.
- Naismith, J.H. and Field, R.A. (1996) Structural basis of trimannoside recognition by concanavalin A. *J. Biol. Chem.*, **271**, 972–976.
- Packer, N.H., Lawson, M.A., Jardine, D.R., and Redmond, J.W. (1998) A general approach to desalting oligosaccharides released from glycoproteins. *Glycoconjugate J.*, **15**, 737–747.
- Patel, T., Bruce, J., Merry, A., Bigge, C., Wormald, M., Jaques, A., and Parekh, R. (1993) Use of hydrazine to release in intact and unreduced form both N- and O-linked oligosaccharides from glycoproteins. *Biochemistry*, **32**, 679–693.
- Pereira, M.E.A. and Kabat, E.A. (1974) Blood group specificity of the lectin from *Lotus tetragonolobus*. *Ann. NY Acad. Sci.*, **234**, 301–305.
- Priem, B., Gitt, R., Bush, A., and Gross, K.C. (1993) Structure of ten free N-glycans in ripening tomato fruit. *Plant Physiol.*, **102**, 445–458.
- Rice, K.G. (2000) Derivatization strategies for preparing N-glycan probes. *Anal. Biochem.*, **283**, 10–16.
- Royle, L., Mattu, T.S., Hart, E., Langridge, J.I., Merry, A.H., Murphy, N., Harvey, D.J., Dwek, R.A., and Rudd, P.M. (2002) An analytical and structural database provides a strategy for sequencing O-glycans from microgram quantities of glycoproteins. *Anal. Biochem.*, **304**, 70–90.
- Rudd, P.M., Guile, G.R., Küster, B., Harvey, D.J., Opdenakker, G., and Dwek, R.A. (1997) Oligosaccharide sequencing technology. *Nature*, **388**, 205–207.
- Rudd, P.M., Mattu, T.S., Masure, T., Van der Steen, P.E., Wormald, M.R., Küster, B., Harvey, D.J., Borregaard, N., Dwek, R.A., and Opdenakker, G. (1999) Glycosylation of natural human neutrophil gelatinase B and neutrophil gelatinase B-associated lipocalin. *Biochemistry*, **38**, 13937–13950.
- Siebert, H.C., Kaptein, R., Beintema, J.J., Soedjanaatmadja, U.M., Wright, C.S., Rice, A., Kleineidam, R.G., Kruse, S., Schauer, R., Pouwels, R.J., Kamerling, J.P., Gabius, H.J., and Vliegthart, J.F.G. (1997) Carbohydrate-protein interaction studies by laser photo CIDNP NMR methods. *Glycoconjugate J.*, **14**, 531–534.
- Starr, C.M., Masada, R.I., Hague, C., Skop, E., and Klock, J.C. (1996) Fluorophore-assisted carbohydrate electrophoresis in the separation, analysis, and sequencing of carbohydrates. *J. Chromatogr. A*, **720**, 295–321.
- Stroop, C.J., Weber, W., Nimtz, M., Gutiérrez Gallego, R., Kamerling, J.P., and Vliegthart, J.F.G. (2000) Fucosylated hybrid-type N-glycans on the secreted human epidermal growth factor receptor from swainsonine-treated A431 cells. *Arch. Biochem. Biophys.*, **374**, 42–51.
- Tseneklidou-Stoeter, D., Gerwig, G.J., Kamerling, J.P., and Spindler, K.-D. (1995) Characterization of N-linked carbohydrate chains of the crayfish, *Astacus leptodactylus* haemocyanin. *Biol. Chem. Hoppe-Seyler*, **376**, 531–537.
- Van Rooijen, J.J.M., Kamerling, J.P., and Vliegthart, J.F.G. (1998) Sulfated di-, tri- and tetraantennary N-glycans in Tamm-Horsfall glycoprotein. *Eur. J. Biochem.*, **256**, 471–487.
- Varki, A. (1993) Biological roles of oligosaccharides: all of the theories are correct. *Glycobiology*, **3**, 97–130.